

Chiral Condensate in Holographic QCD with Baryon Density

Shigenori Seki[†]

Asia Pacific Center for Theoretical Physics

San 31, Hyoja-dong, Nam-gu, Pohang, Gyeongbuk 790-784, Republic of Korea

Sang-Jin Sin[‡]

Department of Physics, Hanyang University, Seoul 133-791, Republic of Korea

Abstract

We consider the chiral condensate in the baryonic dense medium using the generalized Sakai-Sugimoto model. It is defined as the vacuum expectation value of open Wilson line that is proposed to be calculated by use of the area of world-sheet instanton. We evaluate it in confined as well as deconfined phase. In both phases, the chiral condensate has a minimum as a function of baryon density. In the deconfined phase, taking into account the chiral symmetry restoration, we classify the behavior of chiral condensate into three types. One can set the parameter of the theory such that the results, in low but sufficiently higher density, is in agreement with the expectation from QCD.

26 June 2012

[†] sigenori@apctp.org

[‡] sjsin@hanyang.ac.kr

1. Introduction

One of the most important problem in strong interaction physics is the understanding of the chiral symmetry and calculation of its order parameter in dense medium, since it is the key quantity determining the hadron property in the nuclei as well as in neutron stars. For long time, there has been many speculation on the behaviour of chiral condensation in dense medium: one of the intuitively compelling one is that as an order parameter, it is non-zero at vacuum and vanishes at the large enough density where the chiral symmetry is restored. Therefore the most naive but natural behaviour is to decrease as a function of density until it vanishes at the transition point [1]. However, to our knowledge, there is no work which prove this scenario from the first principle. This is because the strongly interacting nature and the presence of the chemical potential have been blocking any reliable calculation even in the numerical approach: the Dyson-Schwinger equation for the resummation is not justified in strong coupling since it involve the truncation of significant part of the diagrams. Furthermore the solution of notorious sign problem in lattice is not available yet.

Since this situation, there have been many activities to utilize the gauge/gravity correspondence [2] to improve the understanding of the nuclear physics. Most notable one is the model of Sakai-Sugimoto [3,4], since the chiral symmetry and its breaking is intuitively realized in geometric way. However, it has its own drawback, since one can not include the quark mass in natural way and calculating chiral condensation is blocked for similar reason. So far, in order to improve this problem, many prescriptions (*e.g.* the uses of tachyonic DBI action [5–8], the introduction of additional D4-branes or D6-branes [9,10], *etc.*) have been suggested. Especially in this paper we are interested in the idea suggested by Aharony and Kutasov [11] to utilize the world-sheet instanton for quark mass and chiral condensation. The idea is to separate the $\bar{\psi}$ and ψ such that one is in D8-branes and the other is in anti-D8-branes in the UV region and covariantize the composite operator by inserting the open Wilson line connecting them. Then the gravity dual of this operator is the world-sheet instanton, a minimal area whose boundary is given by the open Wilson line connecting $\bar{\psi}$ and ψ . This is analogous to the Wilson loop calculation in the closed Wilson line case [12].

The baryons in the Sakai-Sugimoto model are realised as the instantons, in other words, Skyrme-like solitons from the viewpoint of the flavour D8-branes [13], while the baryons are also interpreted to the baryon vertex given by the D4-branes wrapping S^4 ,

which we call baryonic D4-branes [14]. Therefore one can describe the baryonic medium by the use of the baryonic D4-branes which are uniformly distributed in \mathbb{R}^3 [15]. The Sakai-Sugimoto model in dense medium has been attracting many interests [15–18] as well as the other holographic models have [19,20]. In a recent paper, the authors of Ref. [21] worked out the problem of chiral symmetry order parameter in baryonic matter in the context of holographic NJL model [22], which is uncompactified version of Sakai-Sugimoto model, where there is no confinement. In this paper we will work out the calculation in compactified version with confinement.

We will find that we can tune the parameters of the Sakai-Sugimoto model such that chiral condensation decreases as function of density until density reach the chiral transition point, where it suddenly drops to zero. That is, it does not decrease to zero continuously but will go to the first order transition.

The remaining of the paper goes as follows: In Section 2, we review the definition of the generalised Sakai-Sugimoto model [23] and the open Wilson line operator as chiral condensate [11]. In Section 3, we analyse the confined phase. After showing the force balance condition by following Ref. [15], we numerically calculate the chiral condensate, and compare it with the normal nuclear density by the use of the experimental values. In Section 4, in the way similar to the confined phase, we investigate the chiral condensate and the chiral symmetry restoration in the deconfined phase. Section 5 is devoted for the conclusion and discussion.

2. Chiral condensate in generalised Sakai-Sugimoto model

2.1. Generalised Sakai-Sugimoto model

The Sakai-Sugimoto model [3,4] consists of N_c colour D4-branes and N_f pairs of flavour D8-branes and anti-D8-branes. The open strings connecting the D4-branes and the D8-branes (anti-D8-branes) describe quarks (anti-quarks). In large N_c where the AdS/CFT correspondence is valid, we can interpret the colour D4-branes as a background which has two phases.

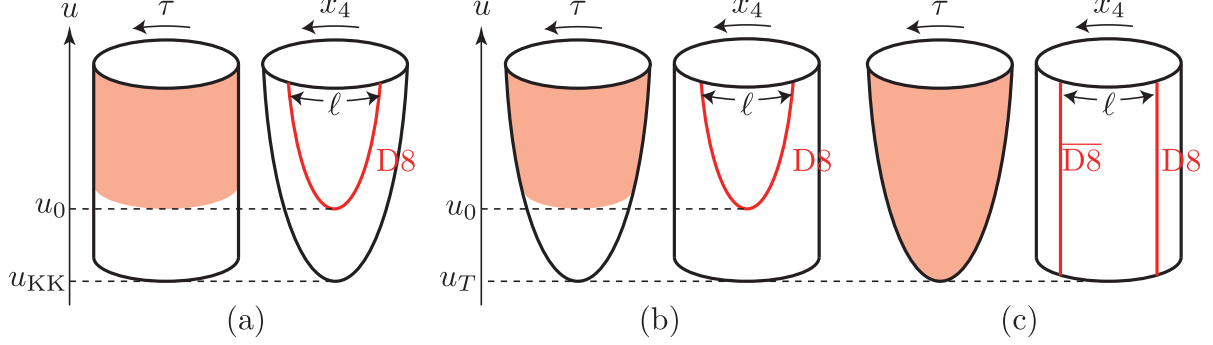


fig. 1 (a) The confined phase where the chiral symmetry is broken.
(b) The deconfined phase where the chiral symmetry is broken.
(c) The deconfined phase where the chiral symmetry is restored.

One is the confined phase (fig. 1a), the other is the deconfined phase (fig. 1b,c). The transition between these two phases is realised as Hawking-Page transition. We can deal with the flavour D8-branes and anti-D8-branes as a probe in this background.

The background (Euclidean) metric in the confined phase is described as

$$R^{-2}ds^2 = u^{\frac{3}{2}} \left[d\tau^2 + \sum_{i=1}^3 (dx_i)^2 + f(u)(dx_4)^2 \right] + u^{-\frac{3}{2}} \left[\frac{du^2}{f(u)} + u^2 d\Omega_4^2 \right], \quad (2.1a)$$

$$e^\phi = g_s u^{\frac{3}{4}}, \quad F_4 = \frac{(2\pi)^3 (\alpha')^{\frac{3}{2}} N_c}{\Omega_4} \epsilon_4, \quad R^3 = \pi g_s N_c (\alpha')^{3/2}, \quad (2.1b)$$

$$f(u) = 1 - \left(\frac{u_{\text{KK}}}{u} \right)^3. \quad (2.1c)$$

Note that the coordinates are dimensionless due to rescaling by the radius R which has a dimension of length. Ω_4 is the volume of a unit S^4 , *i.e.*, $\Omega_4 = 8\pi^2/3$. The D4-branes are originally spanned in the (t, x_1, x_2, x_3, x_4) directions where t is Wick-rotated as $t \rightarrow i\tau$. The x_4 direction is compact with a period β_4 , namely, $x_4 \sim x_4 + \beta_4$. Although generally this yields a conical singularity at $u = u_{\text{KK}}$, one can remove it by choosing

$$\beta_4 = \frac{4\pi}{3} \frac{1}{\sqrt{u_{\text{KK}}}}, \quad (2.2)$$

so that the u - x_4 space has cigar geometry (see fig. 1a). The period β_4 leads to the Kaluza-Klein Mass and the Yang-Mills coupling,

$$M_{\text{KK}} = \frac{2\pi}{R\beta_4}, \quad g_{\text{YM}}^2 = \frac{(2\pi)^2 g_s l_s}{R\beta_4}.$$

Therefore one can obtain the relations between the parameters in the gravity side, R, u_{KK} and g_s , and those in the Yang-Mills theory side, M_{KK} and λ ($:= g_{\text{YM}}^2 N_c$), as follows:

$$R^3 = \frac{\lambda l_s^2}{2M_{\text{KK}}}, \quad u_{\text{KK}} = \frac{2^{\frac{4}{3}}}{9} (\lambda M_{\text{KK}}^2 l_s^2)^{\frac{2}{3}}, \quad g_s = \frac{\lambda}{2\pi N_c M_{\text{KK}} l_s}. \quad (2.3)$$

In order to introduce a temperature in this phase, we compactify the τ direction with a period β_τ , so that the temperature is given by $2\pi/(R\beta_\tau)$.

In the deconfined phase (fig. 1b,c), the background metric is

$$R^{-2} ds^2 = u^{\frac{3}{2}} \left[f_T(u) d\tau^2 + \sum_{i=1}^3 (dx_i)^2 + (dx_4)^2 \right] + u^{-\frac{3}{2}} \left[\frac{du^2}{f_T(u)} + u^2 d\Omega_4^2 \right], \quad (2.4a)$$

$$e^\phi = g_s u^{\frac{3}{4}}, \quad F_4 = \frac{(2\pi)^3 (\alpha')^{\frac{3}{2}} N_c}{\Omega_4} \epsilon_4, \quad R^3 = \pi g_s N_c (\alpha')^{\frac{3}{2}}, \quad (2.4b)$$

$$f_T(u) = 1 - \left(\frac{u_T}{u} \right)^3. \quad (2.4c)$$

This Euclidean metric allows us to consider thermodynamics in the deconfined phase. The τ direction is compactified with a period β_τ , *i.e.*, $\tau \sim \tau + \beta_\tau$, so that the period should be related to u_T as

$$\beta_\tau = \frac{4\pi}{3} \frac{1}{\sqrt{u_T}}, \quad (2.5)$$

by the same reason as (2.2). Then the Hawking temperature T is denoted by $T = 2\pi/(R\beta_\tau)$. By this compactification the τ - u space of the background becomes a cigar (fig. 1b,c). We also compactify the x_4 direction with the period β_4 .

In the backgrounds, (2.1) and (2.4), we consider the flavour D8-branes and anti-D8-branes as a probe. In the confined phase, the D8-branes and anti-D8-branes are connected and become U-shape D8-branes. Since the pair of D8-branes and anti-D8-branes describe $U(N_f)_L \times U(N_f)_R$ chiral symmetry, the U-shape D8-branes imply the chiral symmetry breaking, $U(N_f)_L \times U(N_f)_R \rightarrow U(N_f)$. On the other hand, there are two possibilities in the deconfined phase. One is the chiral symmetry broken phase which is represented by the U-shape D8-branes (fig. 1b). The other is the chiral symmetry restored phase given by the configuration of parallel D8-branes and anti-D8-branes (fig. 1c).

In the original Sakai-Sugimoto model, the D8-branes and anti-D8-branes are placed at the antipodal position in the circle of x_4 direction, in other words, the separation ℓ between the D8-branes at the UV limit, $u = \infty$, is a half of the period of x_4 direction, $\ell = \beta_4/2$. However one can generalise the separation to be any ℓ less than $\beta_4/2$. In this paper we

consider this generalised Sakai-Sugimoto model, to which Bergman *et al.* introduced a baryon density [15].

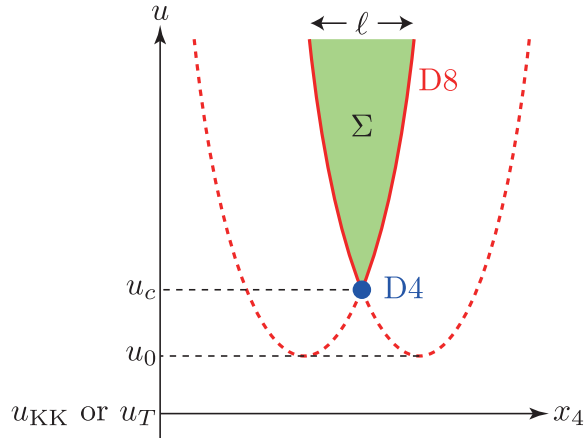


fig. 2 The V-shape D8-branes with baryonic D4-branes. The green shaded region is the world-sheet of string corresponding to the open Wilson line.

The baryons are realised as the D4-branes wrapping S^4 which are located at the tip of the flavour D8-branes. Therefore the system of generalised Sakai-Sugimoto model with baryons should obey the balance condition for the forces between the D4-branes and the D8-branes. This condition gives rise to the modification of the D8-branes from U-shape to V-shape (fig. 2) [15].

2.2. Open Wilson line as chiral condensate

So far many trials for incorporating a chiral condensate into the Sakai-Sugimoto model have been done. In this paper we adopt the method introduced by Aharony and Kutasov [11]. Let us consider the open Wilson line operator,

$$\mathcal{O}_i^j(x^\mu) = \psi_L^{\dagger j} \left(x^\mu, x^4 = -\frac{\ell}{2} \right) \mathcal{P} \exp \left[\int_{-\ell/2}^{\ell/2} (iA_4 + \Phi) dx^4 \right] \psi_{Ri} \left(x^\mu, x^4 = \frac{\ell}{2} \right),$$

where Φ is one of the scalar fields in the super-Yang-Mills theory and i, j are indices of the fundamental representation of $U(N_f)$. This corresponds to the well-known order parameter of chiral symmetry breaking, $\psi_L^{\dagger j} \psi_{Ri}$, in QCD. In the D-brane configuration that we are considering, the operator ψ is at the UV boundary on the V-shape (or U-shape) D8-branes. Therefore, following the AdS/CFT correspondence, one can calculate the vacuum expectation value of \mathcal{O}_i^j ,

$$\langle \mathcal{O}_i^j \rangle \simeq \delta_{ij} \langle \mathcal{O} \rangle, \quad \langle \mathcal{O} \rangle = e^{-S_{\mathcal{O}}},$$

where $S_{\mathcal{O}}$ is the on-shell Euclidean action of the open string whose world-sheet is bounded by the flavour D8-branes (see fig. 2). To leading order in α' , $S_{\mathcal{O}}$ is calculated by the minimal area of the string world-sheet,

$$S_{\mathcal{O}} = \frac{1}{2\pi\alpha'} \int_{\Sigma} d^2\sigma \sqrt{\det g}, \quad (2.6)$$

where Σ is the region surrounded by the flavour D8-branes (see fig. 2). $\langle \mathcal{O} \rangle$ is proportional to $m_q \langle \bar{\psi}\psi \rangle$, and indeed Ref. [11] has shown that $\langle \mathcal{O} \rangle$ naively satisfies the Gell-Mann-Oakes-Renner relation, $m_{\pi}^2 f_{\pi}^2 \propto \langle \mathcal{O} \rangle$.

3. Confined phase

3.1. D-brane configuration and force balance condition

In this subsection, following Ref. [15], we shall show the V-shape solution of flavour D8-branes, the baryonic D4-branes wrapping S^4 and their force balance condition.

We start with the action of the N_f flavour D8-branes embedded in the background (2.1) which have the world-volume coordinates $(\tau, x_1, x_2, x_3, u, \Omega_4)$ and the collective coordinate $x_4(u)$. The world-volume gauge fields on the D8-branes are decomposed into

$$\mathcal{A} = A_{SU(N_f)} + \frac{1}{\sqrt{2N_f}} A_{U(1)}.$$

Since the $U(1)$ part is related with the baryon density that we are here interested in, we turn on

$$a_{\tau}(u) := \frac{2\pi\alpha'}{R^2 \sqrt{2N_f}} A_{U(1),\tau}(u), \quad (3.1)$$

where we assumed that the gauge field depends only on u . Note that the rescaled gauge field $a_{\tau}(u)$ is dimensionless. Then the DBI action of D8-branes is written down as

$$S_8^{(\text{DBI})} = -\mathcal{N} V_3 \int d\tau du \mathcal{L}[x'_4, a'_{\tau}], \quad (3.2a)$$

$$\mathcal{L}[x'_4, a'_{\tau}] = u^4 \sqrt{f(u)(x'_4(u))^2 - \frac{1}{u^3}(a'_{\tau}(u))^2 + \frac{1}{u^3 f(u)}}, \quad (3.2b)$$

where $\mathcal{N} = N_f \mu_8 \Omega_4 R^9 / g_s$ and $V_3 (= \int d^3x)$ is the volume of \mathbb{R}^3 . μ_8 is the D8-brane's tension, *i.e.*, $\mu_8 = (2\pi)^{-8} (\alpha')^{-9/2}$. Note that V_3 is a dimensionless value because the

coordinates of \mathbb{R}^3 , x_i ($i = 1, 2, 3$), are dimensionless. We introduce an electric displacement field $d(u)$ by

$$d(u) := -\frac{\delta\mathcal{L}}{\delta a'_\tau(u)} = ua'_\tau(u) \left[f(u)(x'_4(u))^2 - \frac{1}{u^3}(a'_\tau(u))^2 + \frac{1}{u^3 f(u)} \right]^{-\frac{1}{2}}. \quad (3.3)$$

This will later be associated with the baryon density. In terms of $d(u)$, the equations of motion for $x_4(u)$ and $a_\tau(u)$ from the action (3.2) are expressed as

$$0 = \frac{d}{du} \left[u^4 f(u) x'_4(u) \left(1 + \frac{(d(u))^2}{u^5} \right)^{\frac{1}{2}} \left(f(u)(x'_4(u))^2 + \frac{1}{u^3 f(u)} \right)^{-\frac{1}{2}} \right], \quad (3.4a)$$

$$0 = d'(u). \quad (3.4b)$$

Integrating these equations once with respect to u , we obtain

$$(x'_4(u))^2 = \frac{1}{u^3 (f(u))^2} \left[\frac{f(u)(u^8 + u^3 d^2)}{f(u_0)(u_0^8 + u_0^3 d^2)} - 1 \right]^{-1}, \quad (3.5a)$$

$$d(u) = d, \quad (3.5b)$$

where d and u_0 are integration constants. u_0 is the point at which x'_4 diverges (see fig. 2).

The Chern-Simons action of the D8-branes,

$$S_8^{(\text{CS})} = \frac{\mu_8}{3!} \int C_3 \wedge \text{Tr}(2\pi\alpha' \mathcal{F}')^3 = \frac{N_c}{24\pi^2} \int \omega_5(\mathcal{A}),$$

where $\omega_5(\mathcal{A}) = \text{Tr}(\mathcal{A}\mathcal{F}^2 - 2^{-1}\mathcal{A}^3\mathcal{F} + 10^{-1}\mathcal{A}^5)$, introduces a source of $a_\tau(u)$ at $u = u_c (\geq u_0)$:

$$N_c V_3 \int d\tau du \frac{1}{\sqrt{2N_f}} A_{U(1),\tau} \frac{1}{8\pi^2} \text{tr} F_{SU(N_f)}^2.$$

We assume a uniform distribution of baryons in the \mathbb{R}^3 of x^i ($i = 1, 2, 3$), namely,

$$\frac{1}{8\pi^2} \text{tr} F_{SU(N_f)}^2 = n_4 \delta(u - u_c). \quad (3.6)$$

n_4 implies a baryon density and indeed one can measure the realistic baryon number density n_B with (length) $^{-3}$ dimension by

$$n_B := \frac{n_4}{R^3}. \quad (3.7)$$

n_4 also corresponds to a dimensionless density parameter of baryonic D4-branes wrapping S^4 . By (3.1), the source term can be written as

$$S_8^{(\text{source})} = \frac{N_c R^2 V_3}{2\pi\alpha'} \int d\tau du a_\tau(u) n_4 \delta(u - u_c).$$

Therefore the equation of motion for $a_\tau(u)$ coming from the total action, $S_8^{\text{DBI}} + S_8^{(\text{source})}$, is

$$\mathcal{N}d'(u) = \frac{N_c R^2}{2\pi\alpha'} n_4 \delta(u - u_c).$$

By integrating this with respect to u , the densities, d and n_4 , are related by

$$d = \frac{N_c R^2}{2\pi\alpha' \mathcal{N}} n_4. \quad (3.8)$$

The source of baryon charge can be interpreted as $N_4 (= n_4 V_3)$ baryonic D4-branes wrapping S^4 at $u = u_c$. Since the DBI action of the D4-branes is

$$S_4 = -N_4 \mu_4 \int d\tau d\Omega_4 e^{-\phi} \sqrt{\det g},$$

where $\mu_4 = (2\pi)^{-4} (\alpha')^{-5/2}$, the free energy \mathcal{E}_4 of the on-shell D4-branes wrapping S^4 at $u = u_c$ is given by $S_4|_{\text{on-shell}} =: -\int d\tau \mathcal{E}_4$,

$$\mathcal{E}_4 = \frac{\mathcal{N} V_3}{3} u_c d. \quad (3.9)$$

We now consider the force balance condition between the baryonic D4-branes and the flavour D8-branes. The force of the D4-branes along the u direction at $u = u_c$ is evaluated as

$$f_4 = \frac{1}{\sqrt{g_{uu}}} \Big|_{u=u_c} \frac{d\mathcal{E}_4}{du_c} = \frac{\mathcal{N} V_3}{3R} du_c^{\frac{3}{4}} \sqrt{f(u_c)}. \quad (3.10)$$

Since the Legendre transformation of the D8-branes' action (3.2) with respect to $a_\tau(u)$ becomes

$$\begin{aligned} \tilde{S}_8 &= S_8^{(\text{DBI})} - \mathcal{N} V_3 \int d\tau du d(u) a'_\tau(u) \\ &= -\mathcal{N} V_3 \int d\tau \int_{u_c}^{\infty} du u^4 \sqrt{\left(f(u) (x'_4(u))^2 + \frac{1}{u^3 f(u)} \right) \left(1 + \frac{(d(u))^2}{u^5} \right)}, \end{aligned}$$

we can read the tension of D8-branes at $u = u_c$ under the on-shell condition (3.5),

$$f_8 = \frac{\mathcal{N} V_3}{R} u_c^{\frac{3}{4}} \sqrt{u_c^5 + d^2}, \quad (3.11)$$

while the angle between the u axis and the D8-branes is described as

$$\cos \theta = \frac{\sqrt{g_{uu}} du}{\sqrt{g_{uu} du^2 + g_{44} dx_4^2}} \Big|_{u=u_c} = \sqrt{1 - \frac{f(u_0)(u_0^8 + u_0^3 d^2)}{f(u_c)(u_c^8 + u_c^3 d^2)}}. \quad (3.12)$$

Therefore the force yielded by the D8-branes along the u direction is $f_8 \cos \theta$. Finally, from (3.10), (3.11) and (3.12), the force balance condition, $f_4 = f_8 \cos \theta$, leads to

$$\frac{1}{3}d = \sqrt{\frac{u_c^5 + d^2}{f(u_c)} \left(1 - \frac{f(u_0)(u_0^8 + u_0^3 d^2)}{f(u_c)(u_c^8 + u_c^3 d^2)} \right)}. \quad (3.13)$$

One can show that u_c is related to ℓ , the separation between the D8-branes in the x_4 direction, by

$$\ell = 2 \int_{u_c}^{\infty} du x'_4(u) = 2 \int_{u_c}^{\infty} du \frac{1}{u^{\frac{3}{2}} f(u)} \left[\frac{f(u)(u^8 + u^3 d^2)}{f(u_0)(u_0^8 + u_0^3 d^2)} - 1 \right]^{-\frac{1}{2}}. \quad (3.14)$$

Note that $\ell \leq \beta_4/2$. The $\ell = \beta_4/2$ case corresponds to the original Sakai-Sugimoto model.

3.2. Chiral condensate

In order to evaluate the chiral condensate, we need to compute the area of string instanton world-sheet (2.6),

$$S_{\mathcal{O}} = \frac{R^2}{2\pi\alpha'} \int_{-\ell/2}^{\ell/2} dx_4 \int_{u(x_4)}^{\infty} du = \frac{R^2}{\pi\alpha'} \int_0^{\ell/2} dx_4 \int_{u(x_4)}^{\infty} du.$$

Since there is UV divergence in $S_{\mathcal{O}}$, regularisation is necessary. In Ref. [21] a UV cutoff parameter u_{∞} was introduced, however this regularisation neglects the contribution from the shape of D8-branes in the region of $u > u_{\infty}$. Here we regularise $S_{\mathcal{O}}$ by subtracting a density independent but infinite constant,

$$S_{\infty} := \frac{R^2}{\pi\alpha'} \int_0^{\ell/2} dx_4 \int_{u_{\text{KK}}}^{\infty} du,$$

which is the area supported by two lines, $x_4 = \pm\ell/2$. Then the regularized area $S_{\mathcal{O}}^{\text{reg}}$ is given by

$$S_{\mathcal{O}}^{\text{reg}} := S_{\mathcal{O}} - S_{\infty} = \frac{R^2}{2\pi\alpha'} \ell u_{\text{KK}} - \frac{R^2}{\pi\alpha'} \int_{u_c}^{\infty} du u x'_4(u). \quad (3.15)$$

Then the vacuum expectation value of open Wilson line operator is defined by

$$\langle \mathcal{O} \rangle_{\text{reg}} := e^{-S_{\mathcal{O}}^{\text{reg}}}, \quad (3.16)$$

and it is identified as the chiral condensate $\langle \bar{\psi} \psi \rangle$.

We shall compute it numerically, since computing $S_{\mathcal{O}}^{\text{reg}}$ analytically is not easy. If we rescale the variables as

$$z := \frac{u}{u_{\text{KK}}}, \quad z_0 := \frac{u_0}{u_{\text{KK}}}, \quad z_c := \frac{u_c}{u_{\text{KK}}}, \quad \rho := \frac{d}{u_{\text{KK}}^{5/2}}, \quad \tilde{\ell} := \ell \sqrt{u_{\text{KK}}}, \quad (3.17)$$

then one can exclude the appearance of u_{KK} from the numerical analysis. (3.13) leads to

$$Z_0(z_c, \rho) := (z_0^3 - 1)(z_0^5 + \rho^2) = (z_c^3 - 1)(z_c^5 + \rho^2) \left(1 - \frac{1}{9} \rho^2 \frac{1 - z_c^{-3}}{z_c^5 + \rho^2} \right), \quad (3.18)$$

and (3.14) can be rewritten as

$$\tilde{\ell} = 2 \int_{z_c}^{\infty} dz \frac{z^{3/2}}{z^3 - 1} \left[\frac{(z^3 - 1)(z^5 + \rho^2)}{Z_0(z_c, \rho)} - 1 \right]^{-\frac{1}{2}}. \quad (3.19)$$

$\tilde{\ell}(z_c, \rho)$ is the monotonically decreasing function with respect to z_c for any fixed ρ , and especially $\tilde{\ell}(1, \rho)$ is equal to $\sqrt{u_{\text{KK}}} \beta_4 / 2 = 2\pi/3$, which means the antipodal position. The regularized area (3.15) is

$$S_{\mathcal{O}}^{\text{reg}} = \frac{R^2}{\pi \alpha'} \sqrt{u_{\text{KK}}} G_{\text{conf}}, \quad (3.20a)$$

$$G_{\text{conf}} = - \int_{z_c}^{\infty} dz \frac{z^{3/2}}{z^2 + z + 1} \left[\frac{(z^3 - 1)(z^5 + \rho^2)}{Z_0(z_c, \rho)} - 1 \right]^{-\frac{1}{2}}. \quad (3.20b)$$

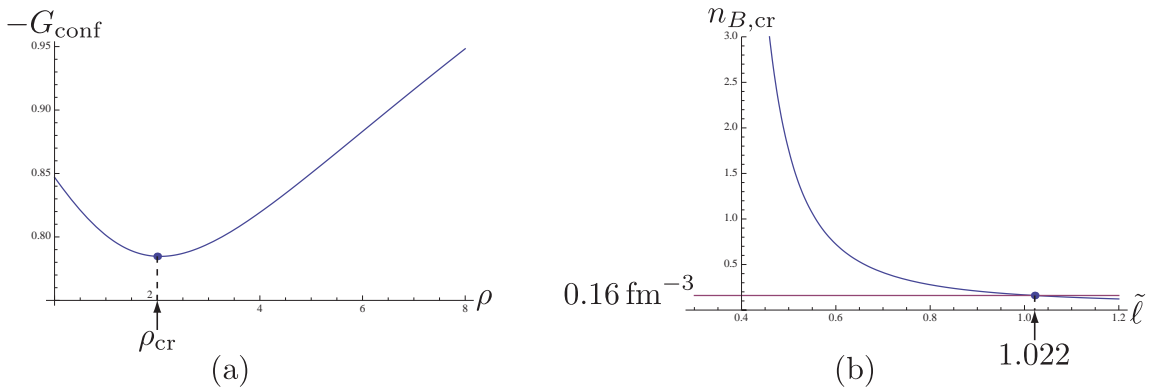


fig. 3 (a) The numerical plot of $-G_{\text{conf}}(\rho)$ with $\tilde{\ell} = 1/2$ fixed.
(b) The critical density $n_{B,\text{cr}}(\tilde{\ell})$.

From now on we set $\tilde{\ell} = 1/2$ for definiteness of our model. The numerical plot of $-G_{\text{conf}}(\rho)$, the regularized area, is depicted by fig. 3a. From this plot, we can find that

$\langle \mathcal{O} \rangle_{\text{reg}}$ becomes minimum at $\rho_{\text{cr}} \approx 2.058$. Setting $N_c = 3$ and $N_f = 2$, we evaluate the baryon number density at $\rho = \rho_{\text{cr}}$ in terms of (3.7) and (3.8), namely,

$$n_B = \frac{N_f M_{\text{KK}}^3 \lambda^2}{1458 \pi^4} \rho. \quad (3.21)$$

Here we are interested in the low density region where the chiral condensate ($\sim \langle \mathcal{O} \rangle_{\text{reg}}$) is expected to decrease. We fix M_{KK} and λ by the use of the generalized Sakai-Sugimoto model at zero density [24,25]. Using the experimental values of the mass of ρ meson, $m_\rho \approx 776$ MeV, and the pion decay constant, $f_\pi \approx 93$ MeV, one can obtain

$$M_{\text{KK}} \approx 496 \text{ MeV}, \quad \lambda \approx 61.7.$$

Note that these values are for the non-antipodal model with $\tilde{\ell} = 1/2$, and different from those in the usual antipodal Sakai-Sugimoto model. Then the number density (3.21) at $\rho_{\text{cr}} \approx 2.058$ is evaluated to be

$$n_{B,\text{cr}} \approx 1.76 \text{ fm}^{-3}.$$

In terms of the normal nuclear density, $n_0 = 0.16 \text{ fm}^{-3}$, we obtain the ratio, $n_{B,\text{cr}}/n_0 \approx 11$, therefore $n_{B,\text{cr}}$ is sufficiently dense.

For any other $\tilde{\ell}$, the behaviour of $\langle \mathcal{O} \rangle_{\text{reg}}$ is schematically same as the case of $\tilde{\ell} = 1/2$, that is to say, the regularized area has minimum at ρ_{cr} as a function of density. Once we choose a model by fixing $\tilde{\ell}$, then ρ_{cr} is determined. $n_{B,\text{cr}}$ calculated from ρ_{cr} through (3.21) is the function of $\tilde{\ell}$, which is depicted by fig. 3b. $n_{B,\text{cr}}$ becomes equal to the normal baryon density at $\tilde{\ell} \approx 1.022$.

4. Deconfined phase

In this section we concentrate on the deconfined phase of the generalised Sakai-Sugimoto model with a baryon density. This phase is similar to the holographic dual of NJL model [22]. Since the fifth direction (x_4) is not compact in the holographic NJL model, the Kaluza-Klein scale M_{KK} does not appear. On the other hand, in our case the x_4 direction is compactified, so that we can compare our results with experimental values by calibrating M_{KK} . The open Wilson line in the holographic NJL model with a baryon density has been studied by Ref. [21], whose analysis is quite similar to ours in the generalised Sakai-Sugimoto model. However we shall use the different regularisation scheme from Ref. [21] in order to include more accurate UV behaviour, and compute physical values by the use of the calibrated M_{KK} and λ .

4.1. D-brane configuration and force balance condition

We turn on the $U(1)$ gauge field defined by (3.1). Then the DBI action of N_f flavour D8-branes in the background (2.4) corresponding to the deconfined phase is

$$S_8^{(\text{DBI})} = -\mathcal{N}V_3\beta_\tau \int du \mathcal{L}[x'_4, a'_\tau], \quad (4.1a)$$

$$\mathcal{L}[x'_4, a'_\tau] = u^4 \sqrt{f_T(u)(x'_4(u))^2 - \frac{1}{u^3}(a'_\tau(u))^2 + \frac{1}{u^3}}. \quad (4.1b)$$

Note that the last term in the square root of (4.1b) is different from that of (3.2b) by the absence of $1/f$ factor. We recall that β_τ is the period of τ direction given by (2.5), therefore the temperature in the deconfined phase is denoted by $T = \beta_\tau^{-1} = (3/4\pi)\sqrt{u_T}$. In the same way as Section 3, we define the electric displacement field by $d(u) \equiv -\delta\mathcal{L}/\delta a'_\tau$ (cf. (3.3)),

$$d(u) = ua'_\tau(u) \left[f_T(u)(x'_4(u))^2 - \frac{1}{u^3}(a'_\tau(u))^2 + \frac{1}{u^3} \right]^{-\frac{1}{2}}. \quad (4.2)$$

Then the equations of motion for $x_4(u)$ and $a_\tau(u)$ are written down as

$$0 = \frac{d}{du} \left[u^4 f_T(u) x'_4(u) \left(1 + \frac{(d(u))^2}{u^5} \right)^{\frac{1}{2}} \left(f_T(u)(x'_4(u))^2 + \frac{1}{u^3 f_T(u)} \right)^{-\frac{1}{2}} \right], \quad (4.3a)$$

$$0 = d'(u). \quad (4.3b)$$

In the deconfined phase, the following constant solution is allowed:

$$x_4(u) = \pm \frac{1}{2}\ell, \quad d(u) = d. \quad (4.4)$$

This describes the parallel D8-branes and anti-D8-branes whose separation is ℓ (see fig. 1c). Therefore (4.4) implies that the chiral symmetry is restored.

One can also find a non-trivial solution of (4.3):

$$(x'_4(u))^2 = \frac{1}{u^3 f_T(u)} \left[\frac{f_T(u)(u^8 + u^3 d^2)}{f_T(u_0)(u_0^8 + u_0^3 d^2)} - 1 \right]^{-1}, \quad (4.5a)$$

$$d(u) = d. \quad (4.5b)$$

This solution corresponds to the V-shape (or U-shape) D8-branes (fig. 1b). From (4.5a) we can calculate the separation between the D8-branes at $u = \infty$,

$$\ell = 2 \int_{u_c}^{\infty} du x'_4(u) = 2 \int_{u_c}^{\infty} du \frac{1}{u^{3/2} \sqrt{f_T(u)}} \left[\frac{f_T(u)(u^8 + u^3 d^2)}{f_T(u_0)(u_0^8 + u_0^3 d^2)} - 1 \right]^{-\frac{1}{2}}. \quad (4.6)$$

The source term comes from the Chern-Simons action of the D8-branes as we explained in Section 3. We assume the uniform distribution of baryons in \mathbb{R}^3 whose density is denoted by n_4 . By integrating the equation of motion for $a_\tau(u)$ which is derived from the DBI action and additionally the source term, the constants d and n_4 are related by (3.8) again in the deconfined phase. The action of $N_4(=n_4V_3)$ baryonic D4-branes wrapping S^4 at $u = u_c$ is calculated as

$$S_4 = -\frac{\mathcal{N}V_3\beta_\tau}{3}du_c\sqrt{f_T(u_c)}, \quad (4.7)$$

and the force generated by these D4-branes along the u direction is evaluated as

$$f_4 = \frac{\mathcal{N}V_3\beta_\tau d}{3R}u_c^{\frac{3}{4}}\left[1 + \frac{1}{2}\left(\frac{u_T}{u_c}\right)^3\right] = \frac{\mathcal{N}V_3\beta_\tau}{2R}du_c^{\frac{3}{4}}\left(1 - \frac{1}{3}f_T(u_c)\right). \quad (4.8)$$

We now compute the force from the flavour D8-branes. From the Legendre transformed action,

$$\tilde{S}_8 = -\mathcal{N}V_3\beta_\tau \int du u^4 \sqrt{\left(f_T(u)(x'_4(u))^2 + \frac{1}{u^3}\right)\left(1 + \frac{(d(u))^2}{u^5}\right)},$$

the tension of the flavour D8-branes is computed to be

$$f_8 = \frac{\mathcal{N}V_3\beta_\tau}{R}u_c^{\frac{3}{4}}\sqrt{f_T(u_c)(u_c^5 + d^2)}. \quad (4.9)$$

Since the angle between the D8-branes and the u axis is

$$\cos\theta = \sqrt{1 - \frac{f_T(u_0)(u_0^8 + u_0^3d^2)}{f_T(u_c)(u_c^8 + u_c^3d^2)}}, \quad (4.10)$$

the force coming from the D8-brane along the u direction becomes $f_8 \cos\theta$. From (4.8), (4.9) and (4.10), we can obtain the force balance condition, $f_4 = f_8 \cos\theta$, that is,

$$\frac{d}{2}\left(1 - \frac{1}{3}f_T(u_c)\right) = \sqrt{f_T(u_c)(u_c^5 + d^2)\left(1 - \frac{f_T(u_0)(u_0^8 + u_0^3d^2)}{f_T(u_c)(u_c^8 + u_c^3d^2)}\right)}. \quad (4.11)$$

4.2. Chiral condensate

We redefine the coordinates by

$$z := \frac{u}{u_T}, \quad z_0 := \frac{u_0}{u_T}, \quad z_c := \frac{u_c}{u_T}, \quad \rho := \frac{d}{u_T^{5/2}}, \quad \tilde{\ell} := \ell\sqrt{u_T}, \quad (4.12)$$

in the similar way to (3.17). Then (4.6) leads to

$$Z_0(z_c, \rho) := (z_0^3 - 1)(z_0^5 + \rho^2) = (z_c^3 - 1)(z_c^5 + \rho^2) \left[1 - \frac{1}{36} \rho^2 \frac{(1 + 2z_c^3)^2}{z_c^3(z_c^3 - 1)(z_c^5 + \rho^2)} \right], \quad (4.13)$$

and one can rewrite (4.11) as

$$\tilde{\ell} = 2 \int_{z_c}^{\infty} dz \frac{1}{\sqrt{z^3 - 1}} \left[\frac{(z^3 - 1)(z^5 + \rho^2)}{Z_0(z_c, \rho)} - 1 \right]^{-\frac{1}{2}}. \quad (4.14)$$

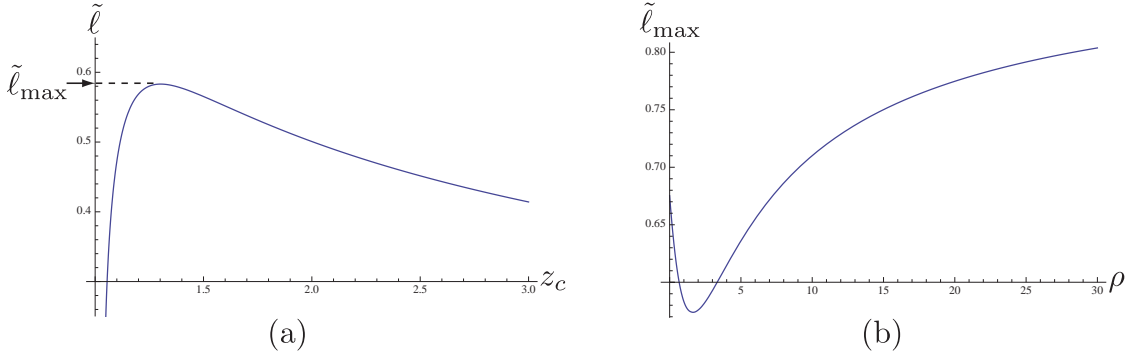


fig. 4 (a) The plot of $\tilde{\ell}$ as function of z_c with $\rho = 1$.
(b) The ρ dependence of $\tilde{\ell}_{\max}(\rho)$.

(4.14) includes three variables, $\tilde{\ell}$, ρ and z_c . As Ref. [15] has pointed out,¹ for any combination of $\tilde{\ell}$ and ρ , z_c does not necessarily exist, because the right hand side of (4.14) with a fixed ρ is the function of z_c , which has a maximum, $\tilde{\ell}_{\max}$ (see fig. 4a). This is a remarkable feature different from the confined phase. By changing ρ , we depict the ρ dependence of $\tilde{\ell}_{\max}$ in fig. 4b. For $\tilde{\ell} > \tilde{\ell}_{\max}$, there is no solution of (4.14), that is, the V-shape solution does not exist, but there is only the parallel solution (4.4). On the other hand, for the opposite case, as one can see from fig. 4a, there are two solutions in z_c of (4.14) for the given value of $\tilde{\ell} (< \tilde{\ell}_{\max})$ and ρ . These two solutions describe different configurations of V-shape D8-branes. *By comparing the free energies for these two configurations, one can clarify that the larger z_c is favoured.* Therefore we hereafter use only the larger z_c .

Let us evaluate the open Wilson line under the constraints given by (4.13) and (4.14). The on-shell world-sheet action of open Wilson line (2.6) in the background (2.4) is

$$S_{\mathcal{O}} = \frac{R^2}{\pi\alpha'} \int_0^{\ell/2} dx_4 \int_{u(x_4)}^{\infty} du \frac{1}{\sqrt{f_T(u)}}.$$

¹ Ref. [15] considered in the variables ℓ and d with fixed temperature. However we here use the rescaled variables (4.12), such that the temperature factor u_T is excluded from the following numerical analyses.

Since this integration diverges by the contribution of UV region, we have to regularise it in the similar manner done in the previous section, that is, we subtract the infinite constant defined by

$$S_\infty := \frac{R^2}{\pi\alpha'} \int_0^{\ell/2} dx_4 \int_{u_T}^\infty du \frac{1}{\sqrt{f_T(u)}}.$$

Since this area is supported by the two parallel lines (4.4), S_∞ is related to “chiral condensate” in the chiral symmetry restoration. We shall give more comments about this issue in Section 5. Then the regularised area becomes

$$S_{\mathcal{O}}^{\text{reg}} = S_{\mathcal{O}} - S_\infty = \frac{R^2}{\pi\alpha'} \sqrt{u_T} G_{\text{deconf}}, \quad (4.15a)$$

$$G_{\text{deconf}} = - \int_{z_c}^\infty dz \left(\int_1^z \frac{d\zeta}{\sqrt{1-\zeta^{-3}}} \right) \frac{1}{\sqrt{z^3-1}} \left[\frac{(z^3-1)(z^5+\rho^2)}{Z_0(z_c, \rho)} - 1 \right]^{-\frac{1}{2}}, \quad (4.15b)$$

where we used (3.16) and (4.13).

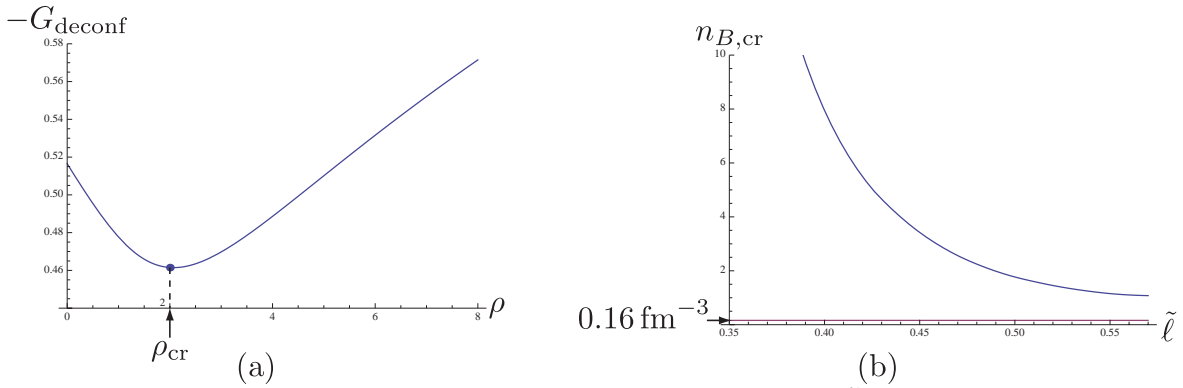


fig. 5 (a) The numerical plot of $-G_{\text{deconf}}(\rho)$ with $\tilde{\ell} = 1/2$ fixed.
(b) The numerical plot of $n_{B,\text{cr}}(\tilde{\ell})$.

Let us set $\tilde{\ell} = 1/2$ for example. The numerical plot of $-G_{\text{deconf}}$ is shown in fig. 5a. It implies that in the deconfined phase also $\langle \mathcal{O} \rangle_{\text{reg}}$ firstly decreases and then increases with respect to the density ρ . $\langle \mathcal{O} \rangle_{\text{reg}}$ has a minimum value at

$$\rho_{\text{cr}} \approx 2.073. \quad (4.16)$$

This is interpreted by the use of (3.21) to the dimensionful value,

$$n_{B,\text{cr}} = 1.771 \text{ fm}^{-3} \approx 11n_0,$$

where we assumed $u_{\text{KK}} = u_T$ for simplicity.²

For arbitrary $\tilde{\ell}$, ρ_{cr} is given by a function of $\tilde{\ell}$. In fig. 5b, we plot $n_{B,\text{cr}}(\tilde{\ell})$ under the assumption of $u_{\text{KK}} = u_T$. The chiral condensate monotonically decreases in the region $n_B < n_{B,\text{cr}}$. A remarkable feature in fig. 5b is that $n_{B,\text{cr}}$ is sufficiently larger than the normal nuclear density.

4.3. Can the chiral symmetry be restored by the density effect?

We have to clarify which solution of the D8-branes is favoured with respect to the baryon density, the parallel configuration (4.4) or the V-shape one (4.5). For this purpose we compare the free energies of these two configurations (*cf.* Ref. [23] in zero density). The energy of the V-shape is given by the flavour D8-branes and the baryon vertex of D4-branes. On the other hand, the energy of the parallel configuration consists of only the D8-branes, because the D4-branes of baryons disappear into the black hole. The discrepancy of the free energies between those configurations is

$$\tilde{S}_8^{(\text{V})} + S_4^{(\text{V})} - \tilde{S}_8^{(\text{parallel})} =: -\mathcal{N}V_3\beta_\tau u_T^{\frac{7}{2}}\Delta\mathcal{E}(\rho; \tilde{\ell}),$$

where

$$\begin{aligned} \Delta\mathcal{E}(\rho; \tilde{\ell}) = & \int_{z_c}^{\infty} dz \sqrt{z^5 + \rho^2} \left[\left(1 - \frac{(z_0^3 - 1)(z_0^5 + \rho^2)}{(z^3 - 1)(z^5 + \rho^2)} \right)^{-\frac{1}{2}} - 1 \right] - \int_1^{z_c} dz \sqrt{z^5 + \rho^2} \\ & + \frac{1}{3}\rho z_c \sqrt{1 - z_c^{-3}}. \end{aligned}$$

Note that there are the overall minus signs in the actions. Therefore, if $\Delta\mathcal{E}$ is positive (negative), then the parallel configuration (the V-shape configuration) is favoured.

² If we consider arbitrary u_{KK} and u_T , we have to take care on the difference of scalings (see (3.17) and (4.12)), $\tilde{\ell}_{(\text{confine})} = \sqrt{u_{\text{KK}}/u_T} \tilde{\ell}_{(\text{deconfine})} (= \ell)$, in calibrating M_{KK} and λ . The decreasing behaviour of $n_{B,\text{cr}}$ schematically does not change.

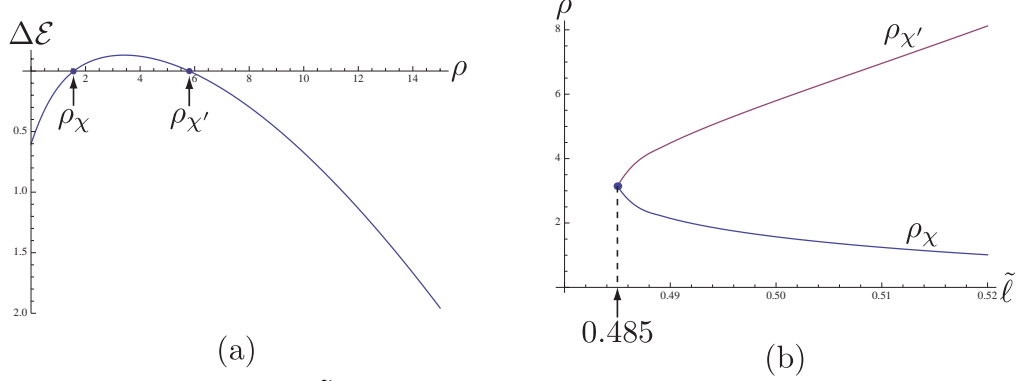


fig. 6 (a) The plot of $\Delta\mathcal{E}(\rho; \tilde{\ell} = 1/2)$, whose zeros are ρ_χ and $\rho_{\chi'}$.
(b) The plots of $\rho_\chi(\tilde{\ell})$ and $\rho_{\chi'}(\tilde{\ell})$. Their crossing point is approximately equal to $(0.485, 3.144)$.

For example, fixing $\tilde{\ell} = 1/2$ again, we compute $\Delta\mathcal{E}(\rho; \tilde{\ell} = 1/2)$. The plot for $\Delta\mathcal{E}(\rho; \tilde{\ell} = 1/2)$ given in fig. 6a shows that $\Delta\mathcal{E}$ has two zeros, namely, the smaller zero, $\rho_\chi \approx 1.571$, and the larger one, $\rho_{\chi'} \approx 5.798$. In the region, $\rho < \rho_\chi$ and $\rho > \rho_{\chi'}$, the chiral symmetry is broken, while in the region, $\rho_\chi < \rho < \rho_{\chi'}$, the chiral symmetry is restored. In the $\tilde{\ell} = 1/2$ model, ρ_χ is smaller than ρ_{cr} (see (4.16)). Therefore the chiral symmetry is restored before the chiral condensate $\langle \mathcal{O} \rangle_{\text{reg}}$ starts to increase. Since one can regard $S_{\mathcal{O}}$ as S_∞ , *i.e.* $S_{\mathcal{O}}^{\text{reg}} = 0$, in the parallel D8-branes solution, the chiral condensate becomes $\langle \mathcal{O} \rangle_{\text{reg}} = 1$ in the chiral symmetry restored phase.

Let us consider an arbitrary $\tilde{\ell}$. The chiral symmetry restoration/breaking points, ρ_χ and $\rho_{\chi'}$, do not necessarily exist for any $\tilde{\ell}$. The $\tilde{\ell}$ dependences of ρ_χ and $\rho_{\chi'}$ are depicted in fig. 6b, which says that ρ_χ and $\rho_{\chi'}$ do not exist when $\tilde{\ell} < 0.485$. In other words, the model with $\tilde{\ell} < 0.485$ does not have the phase of chiral symmetry restoration. On the other hand, in the model with $\tilde{\ell} > 0.485$, the chiral symmetry is restored only in the window region: $\rho_\chi < \rho < \rho_{\chi'}$.

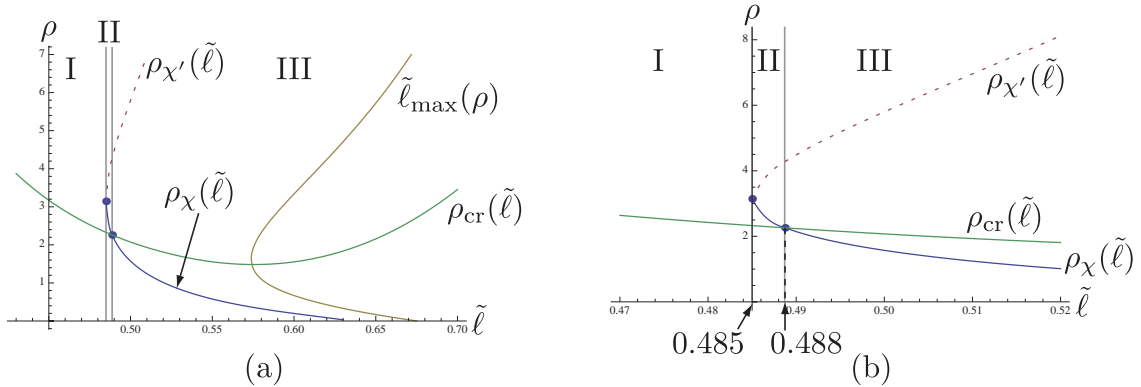


fig. 7 (a) The plots of $\rho_{\text{cr}}(\tilde{\ell})$, $\rho_\chi(\tilde{\ell})$, $\rho_{\chi'}(\tilde{\ell})$ and $\tilde{\ell}_{\text{max}}(\rho)$.
(b) The magnified plot of (a) around the crossing points of ρ_{cr} , ρ_χ and $\rho_{\chi'}$.

Combining $\rho_{\text{cr}}(\tilde{\ell})$, $\rho_{\chi}(\tilde{\ell})$, $\rho_{\chi'}(\tilde{\ell})$ and $\tilde{\ell}_{\text{max}}(\rho)$ that we have calculated so far, we obtain fig. 7. In the region of $\tilde{\ell} > \tilde{\ell}_{\text{max}}$, the chiral symmetry is restored, because there does not exist the V-shape solution but the parallel one. Also in the region of $\tilde{\ell} \gtrsim 0.485$ and $\rho_{\chi} < \rho < \rho_{\chi'}$, the chiral symmetry is restored, because the free energy of the parallel solution is smaller than that of the V-shape solution. In the other region, the chiral symmetry is broken. From fig. 7, we can find the following three types of models on the chiral condensate $\langle \mathcal{O} \rangle_{\text{reg}}$:

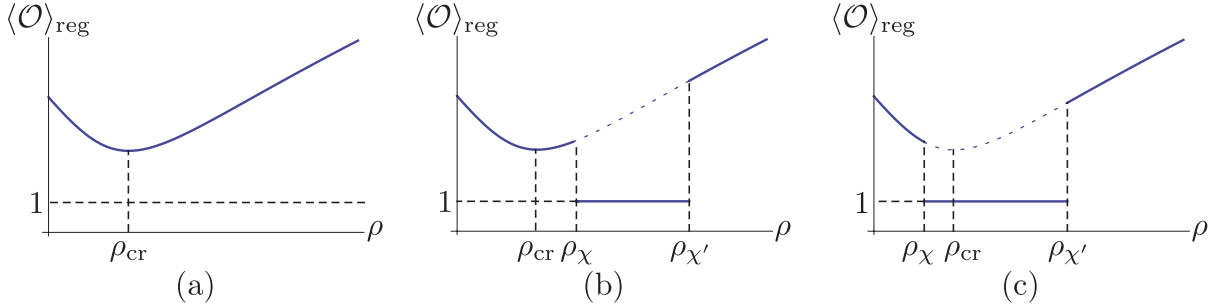


fig. 8 The (regularised) chiral condensate in (a) type I, (b) type II, (c) type III.

I. $\tilde{\ell} < 0.485$

Since the chiral symmetry is always broken, in other words, the chiral symmetry is never restored. $\langle \mathcal{O} \rangle_{\text{reg}}$ firstly decreases and then starts to increase. This is depicted by fig. 8a.

II. $0.485 < \tilde{\ell} < 0.488$

In this type, $\rho_{\text{cr}} < \rho_{\chi} < \rho_{\chi'}$. Therefore the chiral condensate decreases in $\rho < \rho_{\text{cr}}$ and increases in $\rho_{\text{cr}} < \rho < \rho_{\chi}$. In $\rho_{\chi} < \rho < \rho_{\chi'}$ the chiral symmetry is restored, so that $\langle \mathcal{O} \rangle_{\text{reg}}$ is equal to one. When ρ is larger than $\rho_{\chi'}$, the chiral symmetry is broken again. The behaviour of $\langle \mathcal{O} \rangle_{\text{reg}}$ is depicted by fig. 8b.

III. $\tilde{\ell} > 0.488$

Since ρ_{χ} is smaller than ρ_{cr} , before $\langle \mathcal{O} \rangle_{\text{reg}}$ goes up, the chiral symmetry is restored, namely, $\langle \mathcal{O} \rangle_{\text{reg}}$ becomes one. Then in $\rho > \rho_{\chi'}$ the chiral symmetry is broken again and $\langle \mathcal{O} \rangle_{\text{reg}}$ increases. This behaviour is shown in fig. 8c and this case corresponds to the expected result from the field theory intuition.

In models with any $\tilde{\ell}$, $\langle \mathcal{O} \rangle_{\text{reg}}$ almost linearly decreases in low density, and increases at very high density. The type II and type III have the transition to the chiral symmetry restored phase at $\rho = \rho_{\chi}$.

5. Conclusions and discussions

We have studied the chiral condensate given by the open Wilson line in the generalised Sakai-Sugimoto model with the baryon density. In order to exclude u_{KK} and u_T dependences from numerical analyses, we introduced the rescaled variables, (3.17) and (4.12). In both of the confined and deconfined phases, the chiral condensate firstly decreases and then increases with respect to the density ρ (equivalently n_B). We have calculated the critical density $n_{B,\text{cr}}$ at the turning point, which depends on $\tilde{\ell}$. As a result, $n_{B,\text{cr}}$ is the decreasing function of $\tilde{\ell}$. For instance, in the model of $\tilde{\ell} = 1/2$, $n_{B,\text{cr}}$ is about eleven times as large as the normal nuclear density n_0 . Therefore the range, $n_B < n_{B,\text{cr}}$, in which the chiral condensate decreases, is sufficiently large, and this decreasing behaviour agrees with our intuition from ordinary QCD. However the increasing behaviour in very high density is different from the expectation from QCD.

There is not chiral symmetry restoration in the confined phase. On the other hand, in the deconfined phase, there is the region of $\tilde{\ell}$ and ρ in which the chiral symmetry is restored, so that we have found the three types of behaviour of $\langle \mathcal{O} \rangle_{\text{reg}}$ with respect to $\tilde{\ell}$ (see fig. 8). In any types, the decreasing behaviour of $\langle \mathcal{O} \rangle_{\text{reg}}$ in low density is consistent with the results which we expect from the ordinary QCD. In the models of type II and III, there is a transition to the chiral symmetry restoration at $\rho = \rho_\chi$, especially the models in the type III, *i.e.* $\tilde{\ell} > 0.488$, are in good agreement with QCD. However the chiral symmetry restoration occurs before $\langle \mathcal{O} \rangle_{\text{reg}}$ reaches one, that is to say, this transition is in first order.

In all types the chiral condensate grows in very high density, and this behaviour disagrees with our intuition from QCD. A possible problem in the high density is a back-reaction of the baryonic D4-branes. Since the high density means the large number of baryonic D4-branes, the background geometry should be modified by these D4-branes. Ref. [26] has mentioned about such kind of modification. The most honest way to deal with dense baryons in the generalised Sakai-Sugimoto model is to find a classical solution in supergravity with N_c colour D4-branes and N_4 baryonic D4-branes and to deal with the flavour D8-branes as a probe, but this would be difficult.

As we studied so far, the chiral condensate $\langle \mathcal{O} \rangle$ itself defined by the open Wilson line is not appropriate for the order parameter of chiral symmetry. However the positivity of $-\mathcal{S}_{\mathcal{O}}^{\text{reg}}$ by definition, namely, $\langle \mathcal{O} \rangle_{\text{reg}} \geq 1$, is a good tendency to the order parameter. Therefore we suggest the chiral symmetry order parameter χ defined by

$$\chi := \langle \mathcal{O} \rangle_{\text{reg}} - 1 \tag{5.1}$$

so that χ vanishes only when the chiral symmetry is restored: $S_{\mathcal{O}}$ is equal to S_{∞} in the parallel D8-branes and anti-D8-branes configuration. When the chiral symmetry is broken, χ is always positive (see also fig. 8).

Acknowledgment

SS is grateful to Center for Quantum Spacetime (CQeST) in Sogang University and Institut des Haute Études Scientifiques (IHÉS) for hospitality. The work of SJS was supported by Mid-career Researcher Program through NRF grant No. 2010-0008456. It was also partly supported by the National Research Foundation of Korea (NRF) grant through the SRC program CQeST with grant number 2005-0049409.

References

- [1] G. E. Brown and M. Rho, “Scaling effective Lagrangians in a dense medium,” *Phys. Rev. Lett.* **66** (1991) 2720.
- [2] J. M. Maldacena, “The Large N limit of superconformal field theories and supergravity,” *Adv. Theor. Math. Phys.* **2** (1998) 231, [*Int. J. Theor. Phys.* **38** (1999) 1113]. [[hep-th/9711200](#)].
- [3] T. Sakai and S. Sugimoto, “Low energy hadron physics in holographic QCD,” *Prog. Theor. Phys.* **113** (2005) 843. [[hep-th/0412141](#)].
- [4] T. Sakai and S. Sugimoto, “More on a holographic dual of QCD,” *Prog. Theor. Phys.* **114** (2005) 1083. [[hep-th/0507073](#)].
- [5] R. Casero, E. Kiritsis and A. Paredes, “Chiral symmetry breaking as open string tachyon condensation,” *Nucl. Phys. B* **787** (2007) 98. [[hep-th/0702155](#) [[HEP-TH](#)]].
- [6] O. Bergman, S. Seki and J. Sonnenschein, “Quark mass and condensate in HQCD,” *JHEP* **0712** (2007) 037. [[arXiv:0708.2839](#) [[hep-th](#)]].
- [7] A. Dhar and P. Nag, “Tachyon condensation and quark mass in modified Sakai-Sugimoto model,” *Phys. Rev. D* **78** (2008) 066021. [[arXiv:0804.4807](#) [[hep-th](#)]].
- [8] S. Seki, “Intersecting D4-branes model of holographic QCD and tachyon condensation,” *JHEP* **1007** (2010) 091. [[arXiv:1003.2971](#) [[hep-th](#)]].
- [9] K. Hashimoto, T. Hirayama and A. Miwa, “Holographic QCD and pion mass,” *JHEP* **0706** (2007) 020. [[hep-th/0703024](#) [[HEP-TH](#)]].
- [10] K. Hashimoto, T. Hirayama, F. -L. Lin and H. -U. Yee, “Quark mass deformation of holographic massless QCD,” *JHEP* **0807** (2008) 089. [[arXiv:0803.4192](#) [[hep-th](#)]].
- [11] O. Aharony and D. Kutasov, “Holographic duals of long open strings,” *Phys. Rev. D* **78** (2008) 026005. [[arXiv:0803.3547](#) [[hep-th](#)]].
- [12] J. M. Maldacena, “Wilson loops in large N field theories,” *Phys. Rev. Lett.* **80** (1998) 4859. [[hep-th/9803002](#)].
- [13] H. Hata, T. Sakai, S. Sugimoto and S. Yamato, “Baryons from instantons in holographic QCD,” *Prog. Theor. Phys.* **117** (2007) 1157. [[hep-th/0701280](#) [[HEP-TH](#)]].
- [14] E. Witten, “Baryons and branes in anti-de Sitter space,” *JHEP* **9807** (1998) 006. [[hep-th/9805112](#)].
- [15] O. Bergman, G. Lifschytz and M. Lippert, “Holographic nuclear physics,” *JHEP* **0711** (2007) 056. [[arXiv:0708.0326](#) [[hep-th](#)]].
- [16] K. -Y. Kim, S. -J. Sin and I. Zahed, “Dense hadronic matter in holographic QCD,” [[hep-th/0608046](#)].
- [17] K. -Y. Kim, S. -J. Sin and I. Zahed, “The chiral model of Sakai-Sugimoto at finite baryon density,” *JHEP* **0801** (2008) 002. [[arXiv:0708.1469](#) [[hep-th](#)]].
- [18] K. -Y. Kim, S. -J. Sin and I. Zahed, “Dense holographic QCD in the Wigner-Seitz approximation,” *JHEP* **0809** (2008) 001. [[arXiv:0712.1582](#) [[hep-th](#)]].

- [19] S. Nakamura, Y. Seo, S. -J. Sin and K. P. Yogendran, “A new phase at finite quark density from AdS/CFT,” *J. Korean Phys. Soc.* **52** (2008) 1734. [hep-th/0611021].
- [20] Y. Seo and S. -J. Sin, “Baryon mass in medium with holographic QCD,” *JHEP* **0804** (2008) 010. [arXiv:0802.0568 [hep-th]].
- [21] M. Edalati and J. F. Vazquez-Poritz, “Chiral condensates in finite density holographic NJL model from string worldsheets,” [arXiv:0906.5336 [hep-th]].
- [22] E. Antonyan, J. A. Harvey, S. Jensen and D. Kutasov, “NJL and QCD from string theory,” [hep-th/0604017].
- [23] O. Aharony, J. Sonnenschein and S. Yankielowicz, “A Holographic model of deconfinement and chiral symmetry restoration,” *Annals Phys.* **322** (2007) 1420. [hep-th/0604161].
- [24] K. Peeters, J. Sonnenschein and M. Zamaklar, “Holographic melting and related properties of mesons in a quark gluon plasma,” *Phys. Rev. D* **74** (2006) 106008. [hep-th/0606195].
- [25] S. Seki and J. Sonnenschein, “Comments on baryons in holographic QCD,” *JHEP* **0901** (2009) 053. [arXiv:0810.1633 [hep-th]].
- [26] M. Rho, S. -J. Sin and I. Zahed, “Dense QCD: A holographic dyonic salt,” *Phys. Lett. B* **689** (2010) 23. [arXiv:0910.3774 [hep-th]].